SIMPLIFIED SOLAR OPTICAL CALCULATIONS FOR WINDOWS WITH VENETIAN BLINDS

N. A. Kotey and J.L. Wright
Department of Mechanical Engineering, University of Waterloo, 200 University Avenue West, Waterloo, ON Canada, N2L 3G1
Phone: 519-888-4567 ext 3885, Fax: 519-885-5862, Email:nakotey@engmail.uwaterloo.ca

ABSTRACT

Solar gain through a window represents the most variable heat gain imposed on an indoor space. It is also likely to represent the largest heat gain of the indoor space. Shading devices like venetian blinds, roller blinds and drapes are routinely used to control solar gain through windows and their potential for reduction of building load and annual energy consumption is recognized to be large. As such, there is a strong need for models that allow shading layers to be included in glazing system analysis. In this paper, three sets of calculations are presented for a window with light- and dark-coloured venetian blinds using simplified models and computational procedures. For each of the three sets; hourly transmitted, reflected and absorbed fluxes are calculated for both summer and winter conditions. In the first set, the venetian blind is placed on the indoor-side of the window. For the second set, the venetian blind is placed between the glazings. Finally, the third set of results is obtained by placing the venetian blind on the outdoor-side of the window.

INTRODUCTION

Windows with shading devices (complex fenestration systems) are a common occurrence in present day energy efficient buildings. As a first step in energy analysis of complex fenestration systems, short-wave radiation models are used to determine the fraction of incident solar radiation directly transmitted through the complex fenestration system and the fraction that is absorbed in each layer. The absorbed solar energy in each layer then serves as a source term in the second step - heat transfer analysis.

Klems (1994a and 1994b) has recently developed a method to predict the solar gain of complex fenestration systems. The method involves measuring the bi-directional optical properties of a shading layer using a scanning radiometer in order to compile a detailed optical property map of the layer. The properties of the overall complex fenestration system are then built up using matrix layer calculation and the measured layer properties. However, this method is very complex and computationally intensive and hence impractical for building load and annual energy calculations. Klems (1994b) further points out that the use of a bi-directional grid to characterise a non-specular layer with azimuthal dependence requires handling huge matrices with special-purpose computer programs.

EnergyPlus (2005), a building energy analysis software, uses models that calculate the cooling loads of windows with an indoor- or outdoor-side shading device. The models are not applicable to windows with an internal shading device and windows with more than one shading device.

To generalise and simplify the computational procedure for complex fenestration systems of any configuration, a multi-layer solar optical model was developed by Wright and Kotey (2006). The model accounts for both beam and diffuse radiation in the complex fenestration system consisting of specular glazings and non-specular shading layers. It is an extension of an existing solar optical model for specular glazing layers. It is assumed that only specular and/or isotropically diffuse components of solar radiation result from the interaction of insolation with any item in a glazing/shading layer array. An expanded set of solar optical properties is assigned to each layer accordingly. Layers that are not uniform (e.g., venetian blinds, pleated drapes) are assigned spatially averaged, or "effective", solar optical properties. The results of the multi-layer solar optical calculation give the absorbed solar radiation in each layer as well as the transmitted and reflected fluxes.

In order to analyse windows with venetian blinds, Yahoda and Wright (2005), for example, developed an expanded set of optical property models for the blinds using slat geometry and slat surface reflectance. More specifically, the method requires the knowledge of slat surface reflectance as well as its beam-diffuse split. Furthermore, the method requires separate treatment of incident beam and incident diffuse radiation. For incident beam radiation, the method generates both beam-beam and beam-diffuse optical properties. The beam-beam calculations involve tracing specularly reflected rays off the slat surfaces until they emerge from the blind layer. This particular ray tracing technique is computationally intensive as algorithms are required to determine the fraction of incident radiation undergoing a certain number of reflections coupled with a series of geometric conditions imposed on each ray. The beam-diffuse calculations on the other hand involve net radiation analysis which accounts for diffuse reflections off the slat surfaces. The models can therefore be used to calculate solar optical properties pertaining to incident beam and incident diffuse radiation. The models can also be used to obtain both direct-normal and off-normal optical properties of venetian blinds at various slat angles. The models will therefore be useful inputs to the multi-layer glazing/shading solar optical model to analyse windows with venetian blinds. Unfortunately, the models are highly complicated and could result in a lengthy simulation time when integrated into a building energy simulation tool.

In the current study, simplified optical property models of venetian blinds are determined as functions of slat geometry, slat surface optical properties and profile angle of incident beam radiation. More specifically, the slats are assumed to be perfect diffusers and hence transmit and reflect diffusely any incident beam solar radiation. This simplified approach therefore eliminates the computationally intensive ray tracing techniques found in Yahoda's model. It is therefore anticipated that the simplified models will be highly valuable in building energy simulation which places a strong requirement for speed on any of its sub-models.

METHODOLOGY

System Layout and Environmental Conditions

The glazing and shading layers are arranged such that layer (1) is the indoor-side layer while layer (3) is the outdoor-side layer. Figure 1 shows an arrangement of a double-glazed window with an indoor-side venetian blind.

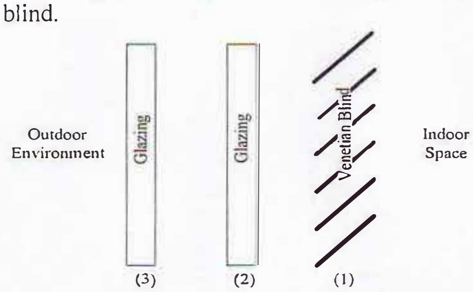

Figure 1. A double-glazed window with an indoor-side venetian blind.

Beam and diffuse components of insolation on the window are estimated using meteorological data from University of Waterloo in conjunction with procedures documented in Duffie and Beckman (1991). The diffuse solar radiation incident on the window is the sum of the diffuse radiation from the sky and ground. The incidence and profile angles are calculated from standard formulae.

Glazing Layer Solar Optical Properties

Solar optical properties of an uncoated glazing layer are functions of wavelength, incidence angle and polarization. Assuming incoming solar radiation is unpolarized; the properties of a glazing layer are calculated by applying Fresnel equations and Snell's Law. Solar optical properties of the glazing for diffuse insolation are obtained by evaluating the corresponding quantity at an incidence angle of 59° (e.g., Duffie and Beckman, 1991).

Venetian Blind Effective Solar Optical Properties

Solar optical properties of a venetian blind layer are determined by considering an enclosure which is representative of an entire blind layer. Figure 2a shows a typical enclosure of a venetian blind where s is the slat separation, w is the slat width and ϕ is the slat angle. The optical properties of the venetian blind are functions of the slat geometry and the slat material optical properties. Optical properties pertaining to beam radiation are also dependent on the profile angle, Ω. Venetian blind optical properties are modelled following a similar methodology described in EnergyPlus (2005). Some simplifications are made to the models by making the following assumptions:

- The slats are flat with negligible thickness
- Incident diffuse radiation is uniformly distributed

The following observations and inherent features of the slats also lead to further simplifications of the models:

- The slats reflect diffusely any incident beam radiation. Measurements show that more than 90% of reflected beam radiation is diffuse (e.g., Parmelee et al., 1953, Breitenbach et al., 2001, Jiang, 2005)
- If the slats are translucent, any incident beam radiation is transmitted diffusely

The optical property models for the venetian blind pertaining to incident beam radiation require the beam-diffuse reflectance of the upward-facing and downward-facing slat surfaces ($\rho^s_{ufs,bd}$ and $\rho^s_{dfs,bd}$) as well as the beam-diffuse transmittance of the slats (τ^s_{bd}). The superscript "s" is attached to the solar optical properties of slats to distinguish them from the effective solar optical properties of the venetian blind. Furthermore, the optical property models for the venetian blind pertaining to incident diffuse radiation require the diffuse-diffuse reflectance of the upward-facing and downward-facing slat surfaces ($\rho^s_{ufs,dd}$ and $\rho^s_{dfs,dd}$) as well as the diffuse-diffuse transmittance of the slats (τ^s_{dd}). From the assumption that slats are perfect diffusers, it follows that $\rho^s_{ufs,bd}$, $\rho^s_{dfs,bd}$ and τ^s_{bd} are independent of the angle of incidence and hence $\rho^s_{ufs,bd} = \rho^s_{ufs,dd}$, $\rho^s_{dfs,bd} = \rho^s_{dfs,dd}$ and $\tau^s_{bd} = \tau^s_{dd}$. Moreover, since there is no beam-beam transmission or reflection (perfectly diffusing slats), $\tau^s_{bb} = 0$, $\rho^s_{ufs,bb} = 0$ and $\rho^s_{dfs,bb} = 0$. Consequently, the only slat material optical properties required as inputs to the blind model are $\rho^s_{ufs,dd}$, $\rho^s_{dfs,dd}$ and τ^s_{dd}.

Beam-Beam Solar Optical Properties

The beam-beam transmittance is the ratio between the beam radiation that passes through the slat openings and the incident beam radiation; this is purely a geometric property. From Figure 2a, the front beam-beam transmittance is

$$\tau_{f,bb} = \frac{s-h}{s} \tag{1}$$

It can be shown that the front beam-beam transmittance is also given by the expression,

$$\tau_{f,bb} = \frac{de-w}{de} \tag{2}$$

where

$$de = s\left|\frac{\cos(\Omega)}{\sin(\Omega+\phi)}\right| \tag{3}$$

Equations (1)-(3) are based on the assumption that the slat thickness is zero. Several correction schemes for slats with finite thickness are available in the literature (e.g., Parmelee and Aubele, 1952, EnergyPlus, 2005). A similar calculation can be used to obtain the back beam-beam transmittance, $\tau_{b,bb}$, by considering beam radiation incident on the back surface of the venetian blind layer.

Beam-Diffuse Solar Optical Properties

The beam-diffuse calculation is subdivided into two categories depending on whether the slats are fully or partially illuminated. For fully illuminated slats, the representative enclosure comprises four surfaces as shown in Figure 2a. Partially illuminated slat surfaces on the other hand give rise to a six-surface enclosure as shown in Figure 2b. The following subsections describe the four- and six-surface models.

Four-Surface Model

As shown in Figure 2a, beam radiation incident on surface w_4 is reflected diffusely into the enclosure. Furthermore, a portion of the beam radiation incident on surface w_4 is diffusely transmitted. Diffuse radiation present within the enclosure will also be transmitted and reflected diffusely by the slats. The following definitions apply:

J_i is the radiosity of surface i, i.e., the radiation flux leaving surface i,

G_i is the irradiance on surface i which is the radiation flux incident on surface i,

Z_i is the diffuse source term due to incident beam radiation on surface i.

From the definitions of J, G, and Z, the following equations can be written:

$$J_3 = Z_3 + \rho^s_{dfs,dd} G_3 + \tau^s_{dd} G_4 \tag{4}$$

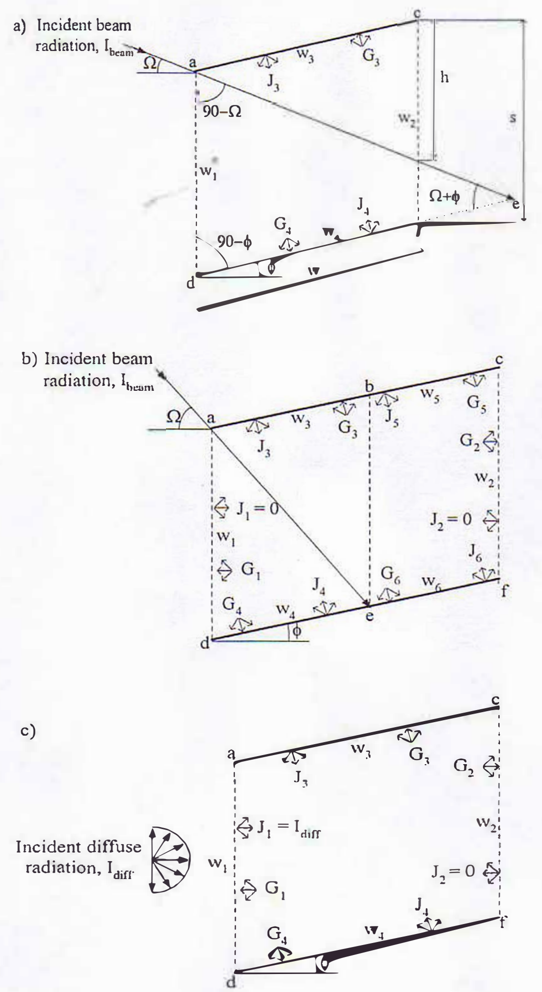

Figure 2. Enclosure Geometry for Calculating Venetian Blind Layer Optical Properties a) Incident Beam Radiation (four-surface model) b) Incident Beam Radiation (six-surface model) c) Incident Diffuse Radiation.

$$J_4 = Z_4 + \tau^s_{dd} G_3 + \rho^s_{ufs,dd} G_4 \tag{5}$$

$$G_i = \sum_{j=1}^{4} F_{ij} J_j \qquad i = 1, 4 \tag{6}$$

The view factor, F_{ij}, is the fraction of diffuse radiation leaving surface i that is intercepted by surface j. The view factors can be determined by Hottel's crossed string rule.

Since there is no incident diffuse radiation at the front and back surfaces of the enclosure, the source terms, $J_1 = J_2 = 0$. The diffuse source terms, Z_3 and Z_4 can be computed for two different cases:

If incident beam radiation, I_{beam}, hits the upward-facing slat surfaces, then

$$Z_3 = \tau^s_{dd} \frac{s}{de} I_{beam} \tag{7}$$

$$Z_4 = \rho^s_{ufs,dd} \frac{s}{de} I_{beam} \quad (8)$$

On the other hand, if incident beam radiation hits downward-facing slat surfaces, then

$$Z_3 = \rho^s_{dfs,dd} \frac{s}{de} I_{beam} \quad (9)$$

$$Z_4 = \tau^s_{dd} \frac{s}{de} I_{beam} \quad (10)$$

Equations (4)-(6) are solved to obtain all the J_j terms. For the purpose of solving equations (4)-(6), I_{beam} is set to unity and the front beam-diffuse transmittance and reflectance of the blind layer are:

$$\tau_{f,bd} = G_2 \quad (11)$$

$$\rho_{f,bd} = G_1 \quad (12)$$

Six-Surface Model

Each slat surface is divided into two segments in order to distinguish between the illuminated and shaded portions of the slat with respect to beam radiation. Following a similar methodology described for the four-surface model, the following equations are written for the six-surface model:

$$J_3 = Z_3 + \rho^s_{dfs,dd} G_3 + \tau^s_{dd} G_4 \quad (13)$$

$$J_4 = Z_4 + \tau^s_{dd} G_3 + \rho^s_{ufs,dd} G_4 \quad (14)$$

$$J_5 = Z_5 + \rho^s_{dfs,dd} G_5 + \tau^s_{dd} G_6 \quad (15)$$

$$J_6 = Z_6 + \tau^s_{dd} G_5 + \rho^s_{ufs,dd} G_6 \quad (16)$$

$$G_i = \sum_{j=1}^{6} F_{ij} J_j \qquad i = 1, 6 \quad (17)$$

Since there is no incident diffuse radiation at the front and back surfaces of the enclosure, the source terms, $J_1 = J_2 = 0$. Also, for the configuration shown in Figure 2b, surfaces w_5 and w_6 are shaded from beam radiation and therefore the source terms, $Z_5 = Z_6 = 0$. The diffuse source terms, Z_3 and Z_4 are computed using equations (7)-(10). After solving equations (13)-(17) for all the J_j terms, the front beam-diffuse transmittance and reflectance are calculated from equations (11) and (12).

A similar analysis is used to determine the back beam-diffuse transmittance and reflectance of the blind by considering beam radiation incident on surface w_2 in Figures 2a and 2b.

Diffuse-Diffuse Solar Optical Properties

The diffuse-diffuse transmittance and reflectance of the blind are calculated using the four-surface model shown in Figure 2c. For a uniformly distributed diffuse radiation incident on the front surface of the enclosure, I_{diff}, the following equations can be written:

$$J_1 = I_{diff} \quad (18)$$

$$J_2 = 0 \quad (19)$$

$$J_3 = \rho^s_{dfs,dd} G_3 + \tau^s_{dd} G_4 \quad (20)$$

$$J_4 = \tau^s_{dd} G_3 + \rho^s_{ufs,dd} G_4 \quad (21)$$

$$G_i = \sum_{j=1}^{4} F_{ij} J_j \qquad i = 1, 4 \quad (22)$$

Equations (18)-(22) are solved to obtain all the J_j terms. For the purpose of solving equations (18)-(22), I_{diff} is set to unity and the front diffuse-diffuse transmittance and reflectance are:

$$\tau_{dd} = G_2 \quad (23)$$

$$\rho_{f,dd} = G_1 \quad (24)$$

The back diffuse-diffuse reflectance is calculated in a similar manner by setting $J_2 = I_{diff} = 1$ and $J_1 = 0$.

Ideally, the optical property calculations for the venetian blind described above must be performed for every wavelength required by the corresponding optical properties of the slat surfaces. However, for the sake of simplicity, the solar (spectrally-averaged) optical properties of the slat surfaces are used.

Multi-layer Calculation

Table 1 summarises the list of solar optical properties of glazing layers and venetian blind required as input to the multi-layer calculation. The cross in each cell in Table 1 indicates the calculated optical properties. Beam-beam reflectances of the venetian blind must be equal to zero. Beam-diffuse properties of specular glazing layers are equal to zero since incident beam radiation leaves a specular glazing layer without being scattered. Having obtained all the solar optical properties of interest, the multi-layer solar optical model (Wright and Kotey, 2006) was used to determine the portions of reflected, transmitted and absorbed solar radiation – including locations of the absorbed amounts in the double-glazed window with the venetian blind. Table 2 summarises the list of output variables generated from the multi-layer calculation.

RESULTS AND DISCUSSION

The windows analysed is this study are assumed to be located in Waterloo, Ontario (latitude 43.5^0 and longitude 80.6^0 west). All the windows are south-facing and are mounted vertically. The meteorological data for typical summer and winter conditions were taken from University of Waterloo weather files on January 01, 2004 and July 01, 2004, respectively. With a fresh snow cover on January 01, 2004, the ground reflectance, ρ_{gr} is assumed to be equal to 0.6. On the other hand, ρ_{gr} is assumed to be equal to 0.2 on July 01, 2004. Figures 3 and 4 show the hourly beam (*GBM*) and diffuse (*GDF*) irradiance on the window for the summer and the winter day, respectively.

Table 1. Summary of solar optical properties of glazing layers and venetian blind.

Solar Optical Property		Glazing Layers	Venetian Blind
$\rho_{f,bb}$	Beam-beam reflectance, front side	X	0
$\rho_{b,bb}$	Beam-beam reflectance, back side	X	0
$\tau_{f,bb}$	Beam-beam transmittance, front side	X	X
$\tau_{b,bb}$	Beam-beam transmittance, back side	X	X
$\rho_{f,bd}$	Beam-diffuse reflectance, front side	0	X
$\rho_{b,bd}$	Beam-diffuse reflectance, back side	0	X
$\tau_{f,bd}$	Beam-diffuse transmittance, front side	0	X
$\tau_{b,bd}$	Beam-diffuse transmittance, back side	0	X
$\rho_{f,dd}$	Diffuse-diffuse reflectance, front side	X	X
$\rho_{b,dd}$	Diffuse-diffuse reflectance, back side	X	X
τ_{dd}	Diffuse-diffuse transmittance	X	X

Table 2. List of output variables generated from the multi-layer calculation.

Symbol	Description
TRANSBB_SYS	Beam-beam transmitted flux through the system (W/m^2)
TRANSBD_SYS	Beam-diffuse transmitted flux through the system (W/m^2)
TRANSDD_SYS	Diffuse-diffuse transmitted flux through the system (W/m^2)
TRANS_SYS	Total (beam plus diffuse) transmitted flux through the system (W/m^2)
REFL_SYS	Total (beam plus diffuse) reflected flux (W/m^2)
S(1)	Absorbed flux in layer 1 - i.e. indoor-side (W/m^2)
S(2)	Absorbed flux in layer 2 (W/m^2)
S(3)	Absorbed flux in layer 3 (W/m^2)

The glazing layers optical properties are calculated using 3-mm clear glass with an index of refraction, n = 1.526 and an extinction coefficient, K = 33.3 m^{-1}. The venetian blind effective optical properties are calculated using simplified models described above. The slat width, the slat spacing and the slat angle are w = 14.8 mm, s = 12.3 mm and ϕ = 10^0, respectively. The light-coloured blind has slat surface reflectivity ($\rho^{s}_{ufs,dd}$ and $\rho^{s}_{dfs,dd}$) of 0.126 while the dark-coloured blind has a surface reflectivity of 0.673 (Jiang, 2005). Both blinds have opaque slats.

Figure 5 compares the hourly transmitted and reflected fluxes for the window with light-coloured indoor-side, between-the-pane and outdoor-side blinds on a summer day (July 01, 2004). The transmitted and reflected fluxes in all three cases follow the same general trend during the day. However, the indoor- side blind configuration shows a slightly elevated beam-diffuse transmitted flux around midday thereby raising the system transmitted flux during that period.

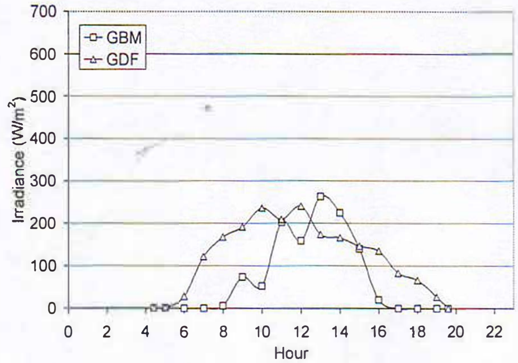

Figure 3. Hourly beam and diffuse irradiance on a south facing window on a summer day (July 01, 2004) in Waterloo, Ontario.

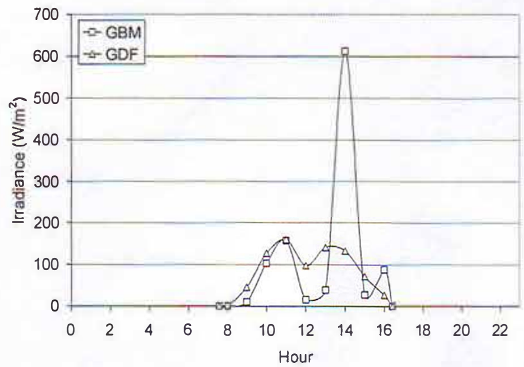

Figure 4. Hourly beam and diffuse irradiance on a south facing window on a winter day (January 01, 2004) in Waterloo, Ontario.

Figure 6 compares the hourly transmitted and reflected fluxes for the window with dark-coloured blinds. As expected, installing dark-coloured blind on the window results in lower transmitted fluxes throughout the day. It is also interesting to note that when the dark-coloured blind is placed at the outdoor-side of the window, the system reflectance is reduced significantly. Figure 7 compares the hourly absorbed fluxes in each layer of the window with light-coloured indoor-side, between-the-pane and outdoor-side blinds on the summer day. Generally, the venetian blind absorbs more solar radiation than the glazing layers although the indoor-side blind hourly absorbed fluxes are comparable to those of the glazing layers for the light-coloured blind (see Figure 7a). The outdoor- side blind, on the other hand, has much higher hourly absorbed fluxes compared to the glazing layers. A similar trend of layer absorbed fluxes is depicted in Figure 8 for the window with dark-coloured blinds. However, the outdoor-side blind has significantly higher hourly absorbed fluxes throughout the day as compared to the glazing layers (see Figure 8c).

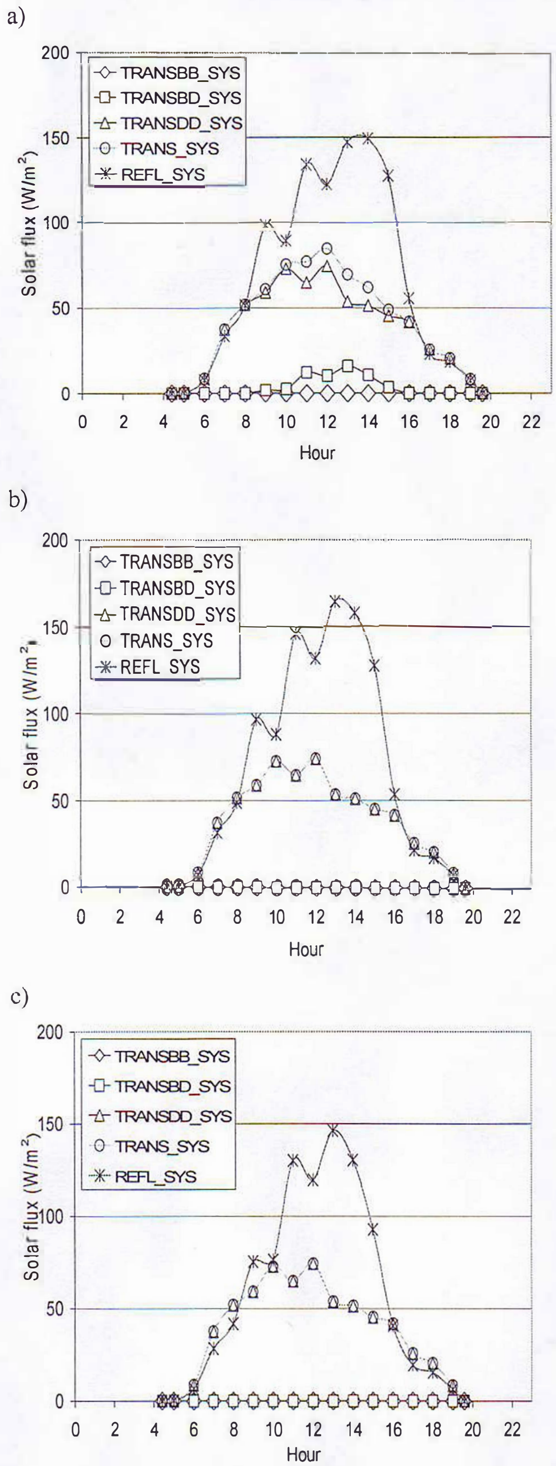

Figure 5. Hourly transmitted and reflected fluxes for the window with light-coloured blind on a summer day (July 01, 2004) - a) Indoor-side blind b) Between-the-pane blind c) Outdoor-side blind.

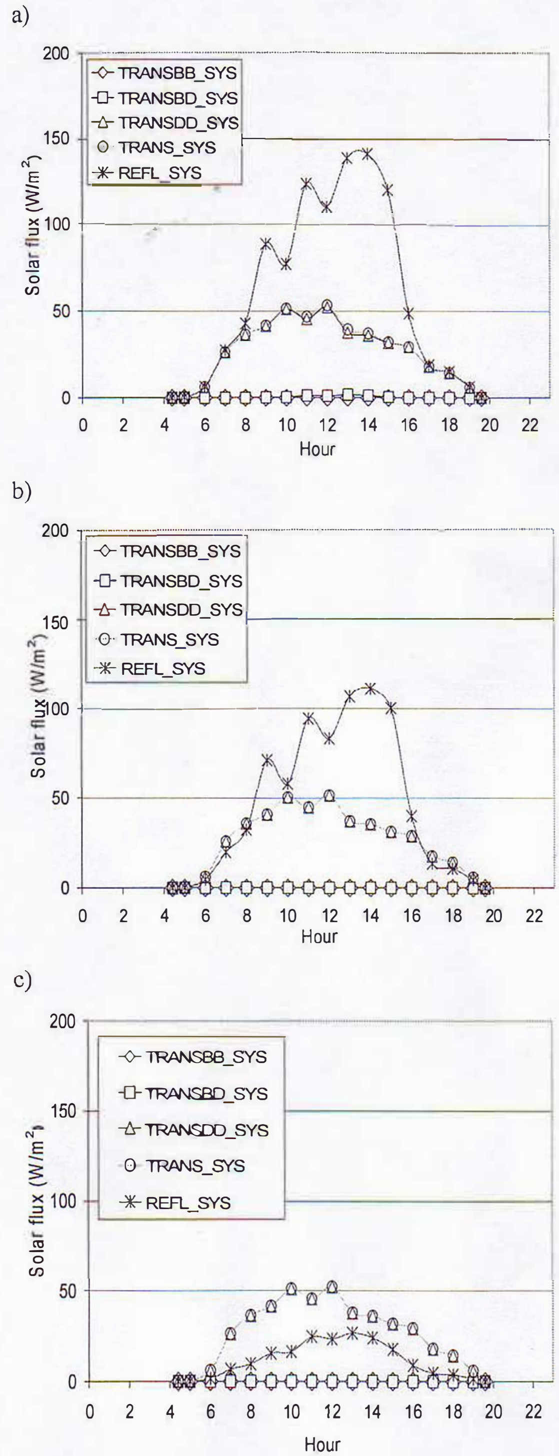

Figure 6. Hourly transmitted and reflected fluxes for the window with dark-coloured blind on a summer day (July 01, 2004) - a) Indoor-side blind b) Between-the pane blind c) Outdoor-side blind.

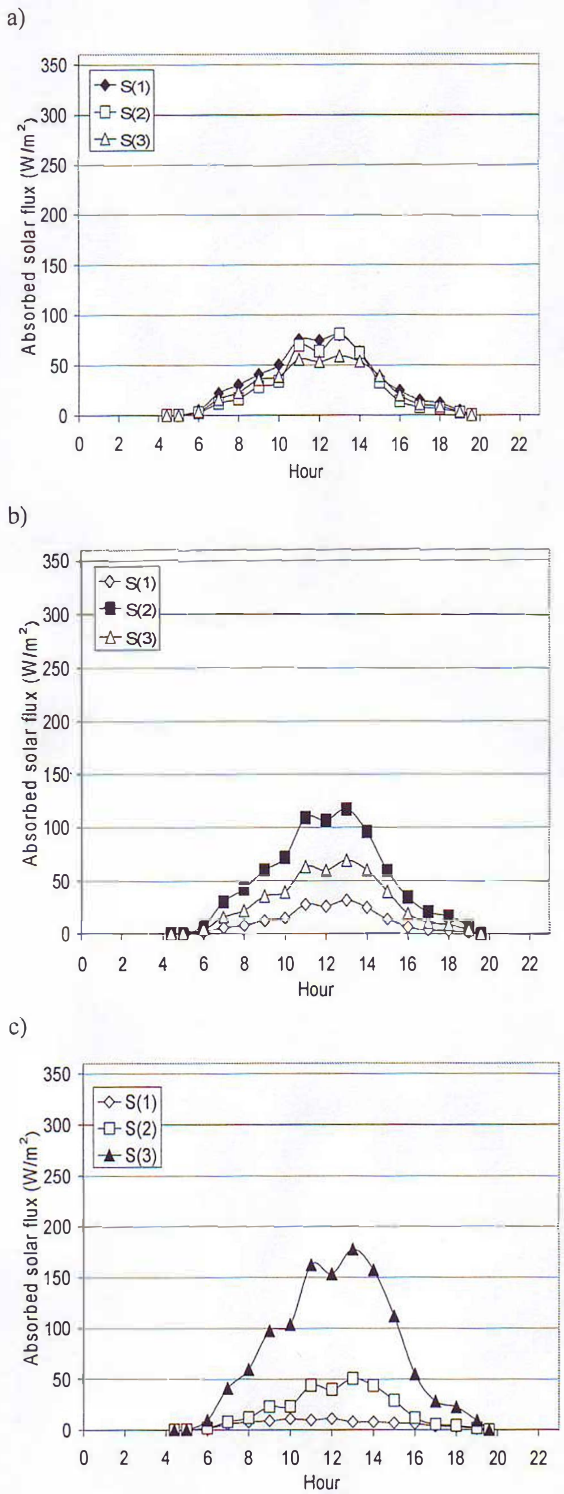

Figure 7. Hourly absorbed fluxes in each layer of the window with light-coloured blind on a summer day (July 01, 2004) – a) Indoor-side blind b) Between-the-pane blind c) Outdoor-side blind.

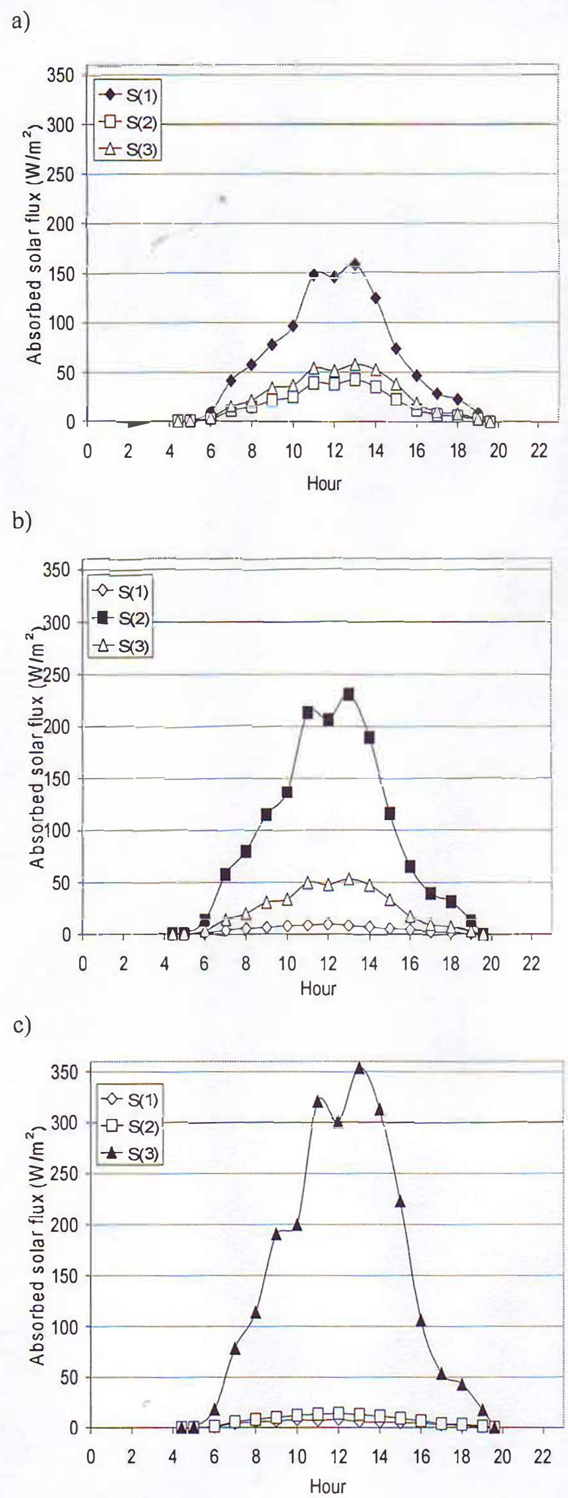

Figure 8. Hourly absorbed fluxes in each layer of the window with dark-coloured blind on a summer day (July 01, 2004) - a) Indoor-side blind b) Between-the-pane blind c) Outdoor-side blind.

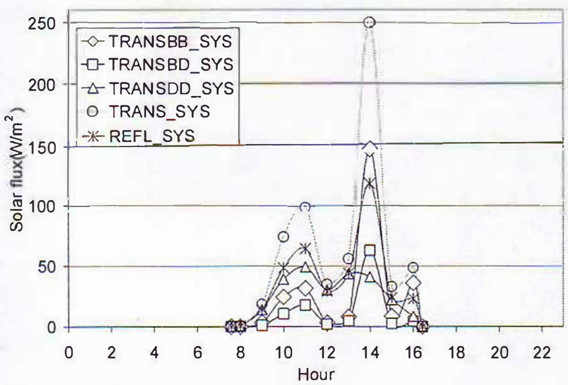

Figure 9. Hourly transmitted and reflected fluxes for the window with light-coloured blind on a winter day(January 01, 2004)

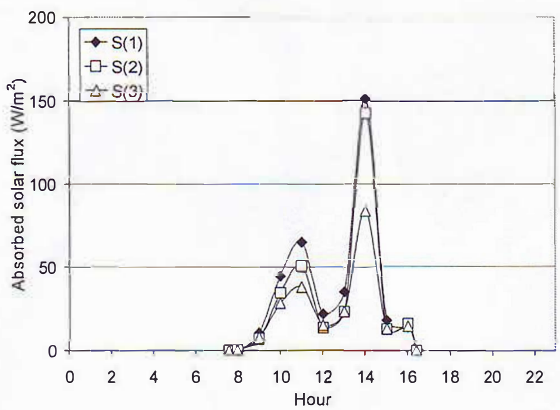

Figure 10. Hourly absorbed fluxes in each layer of the window with light-coloured blind on a winter day (January 01, 2004)

Hourly transmitted, reflected and absorbed fluxes are also calculated for the window with indoor-side, between-the-pane and outdoor-side blinds on a winter day (January 01, 2004). Figures 9 and 10 show graphs for the window with the light-coloured blind placed on the indoor-side of the window. The graphs show peak values of all the fluxes at the 14th hour which is consistent with the beam irradiance at that hour (see Figure 4). It is also interesting to note that the winter graphs depict the same trend as the summer graphs. However, the beam-beam transmitted fluxes for the winter day are generally much higher than those for the summer day. This means that the slat angle chosen for this study allows more solar radiation to be directly transmitted to the indoor space on the winter day than the summer day. Thus, the window configuration chosen in this study might save energy by reducing the cooling and heating loads in the summer and winter, respectively.

CONCLUSIONS

The importance of modelling complex fenestration systems in annual energy simulation programs lies in the need to predict the energy savings potential for various shading devices. In the current study, simplified models are used to calculate the transmitted, reflected and absorbed fluxes of solar radiation for windows with venetian blinds. It is seen from this study that a particular configuration of a window with a venetian blind can significantly influence the amount of energy transmitted to the indoor space at different times of the year. Moreover, the slat angle chosen in this study might reduce the building energy requirements during the summer and winter seasons. The simplified calculation procedures therefore produce results that can serve as useful input to building load and annual energy calculation tools. Furthermore, simplified calculation procedures have advantages especially in the design stages when one wishes to compare the performance of various complex fenestration system configurations.

ACKNOWLEDGMENTS

The research was supported by Natural Sciences and Engineering Council (Canada)

REFERENCES

Breitenbach, J., Lart, S., Langle, I., and Rosenfeld, J.L.J., 2001. Optical and Thermal Performance of Glazing with Integral Venetian Blinds. Energy and Buildings, vol. 33, pp. 433-442.

Duffie, J.A., and Beckman, W.A., 1991. Solar Engineering of Thermal Processes. 2nd edition, John Wiley and Sons Inc.

EnergyPlus, 2005. EnergyPlus Engineering Reference – The Reference to EnergyPlus Calculations. U.S. Department of Energy, pp. 151-169.

Jiang, T., 2005. Transmittance Measurements of Louvered Blinds Using a Broad Area Illumination Integrating Sphere. MASc. Thesis, University of Waterloo, Waterloo, Ontario.

Klems, J.H., 1994a. A New Method for Predicting the Solar Heat Gain of Complex Fenestration System – 1. Overview and Derivation of the Matrix Layer Calculation. ASHRAE Transactions, vol. 100, Part 1, pp. 1065-1072.

Klems, J.H., 1994b. A New Method for Predicting the Solar Heat Gain of Complex Fenestration System – 2. Detailed Description of the Matrix Layer Calculation. ASHRAE Transactions, vol. 100, Part 1, pp. 1073-1086.

Parmelee, G.V., and Aubele, W.W., 1952. The Shading of Sunlit Glass - An Analysis of the Effect of Uniformly Spaced Flat Opaque Slats. ASHVE Transactions, vol. 58, pp. 377-398.

Wright, J.L., and Kotey, N.A., 2006. Solar Absorption by Each Element in a Glazing/Shading Layer Array. ASHRAE Transactions, vol. 112, Part 2.

Yahoda, D.S., and Wright, J.L., 2005. Methods for Calculating the Effective Solar-Optical Properties of a Venetian Blind Layer. ASHRAE Transactions, vol. 111, Part 1, pp. 572-586.